Supporting Information:

Development of QM/MM(ABEEM) Method for the Deprotonation of Neutral and Cation Radicals in G-tetrad and GGX(8-oxo-G) Tetrad

Yue Wang,‡ Linlin Liu,‡ Yue Gao, Jiayue Zhao, Cui Liu,* Lidong Gong,* Zhongzhi Yang

School of Chemistry and Chemical Engineering, Liaoning Normal University, Dalian, 116029, People's Republic of China

Corresponding authors E-mail address:

liuc@lnnu.edu.cn (Cui Liu)

gongjw@lnnu.edu.cn (Lidong Gong)

Tel: +86 411-82158977

Index **page**

1 The hydrogen bond fitting functions of H_2O-H_2O and H_3O^+-H_2O, ABEEM PFF labels of 8-oxo-$G^{\bullet+}$ in GGX(8-oxo-G) tetrad, the linear correlations of charge distributions of $G^{\bullet+}$ in G-tetrad and $X^{\bullet}$ in GGX(8-oxo-G) tetrad calculated by QM/MM(ABEEM) and QM methods

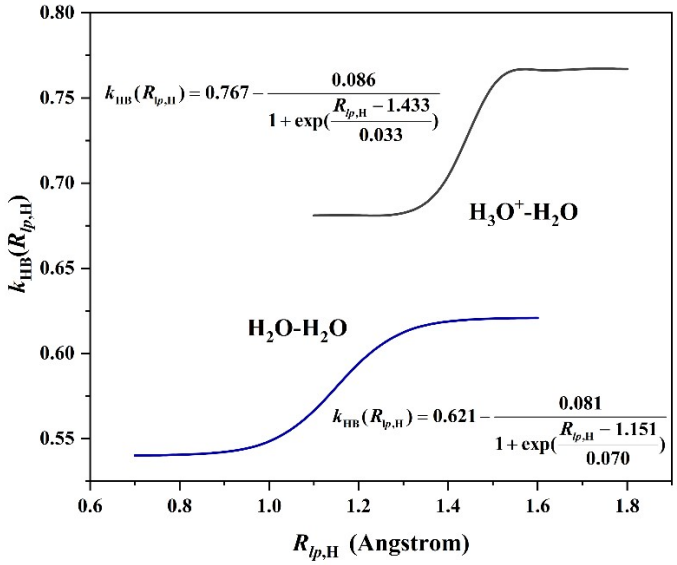

Fig. S1 The different types of hydrogen bonds between water molecules (H_2O-H_2O and H_3O^+-H_2O) are fitted by the distance ($R_{lp,H}$) between the *lp* electrons of the O atom and H atom.

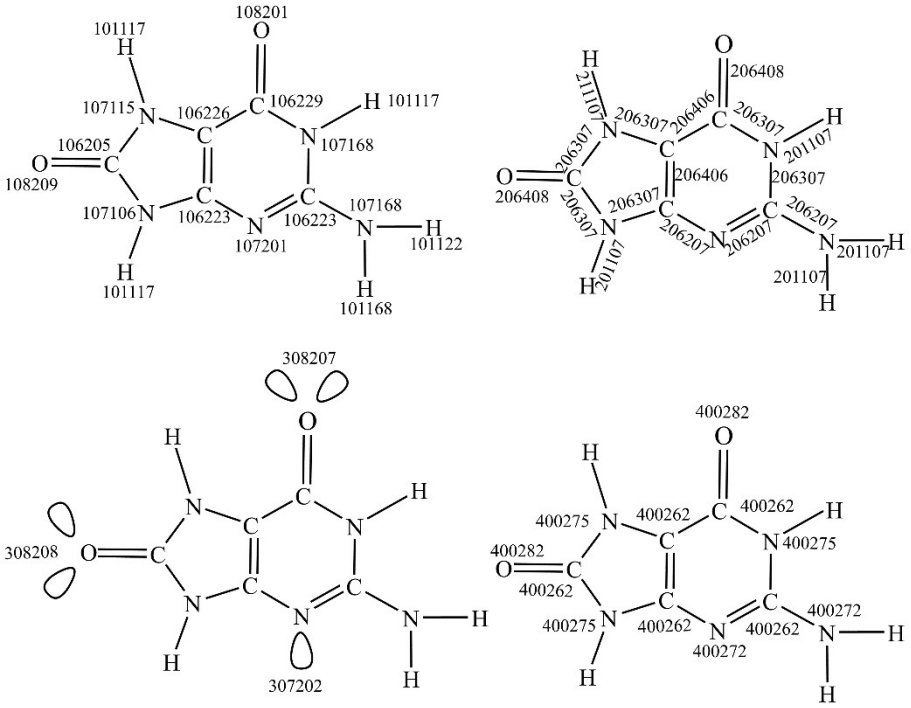

Fig. S2 The ABEEM PFF label of each site of 8-oxo-G$^{\bullet+}$ in GGX(8-oxo-G) tetrad. The six digits beginning with 1 represent the atom site, the number beginning with 2 represents the σ bond site, the number beginning with 3 represents the *lp* electrons site, and the number beginning with 4 represents the π bond site.

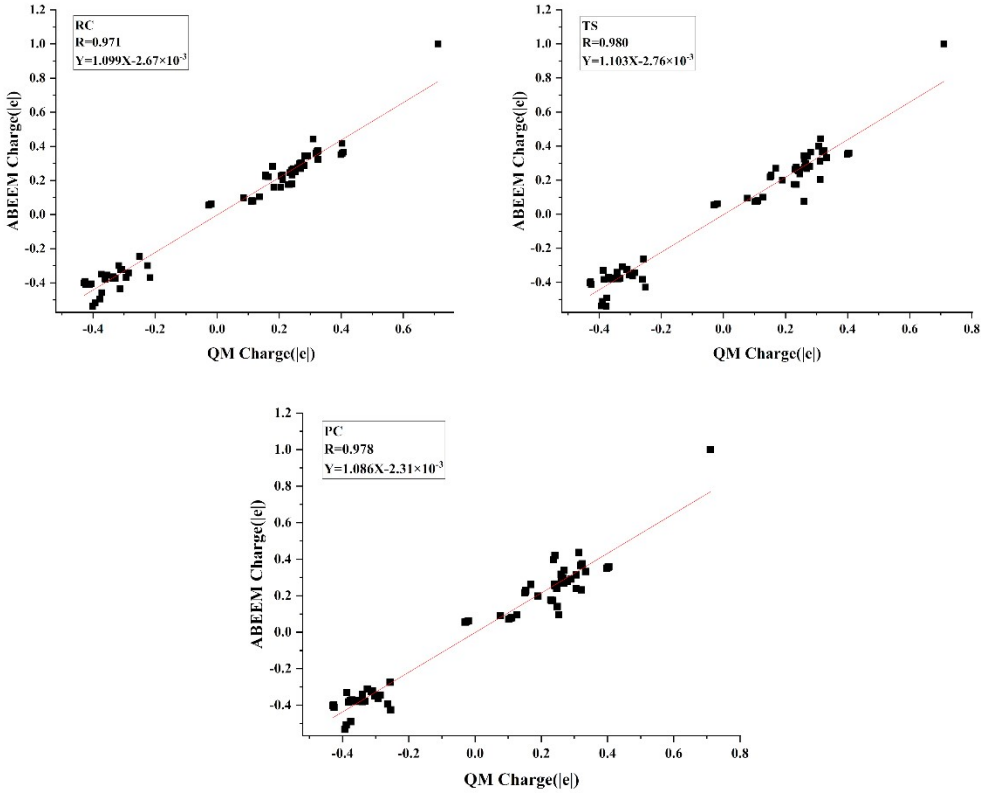

Fig. S3 The linear correlations of charge distributions of RC, TS and PC during deprotonation of $G^{\bullet+}$ in G-tetrad obtained by QM/MM(ABEEM) and QM methods.

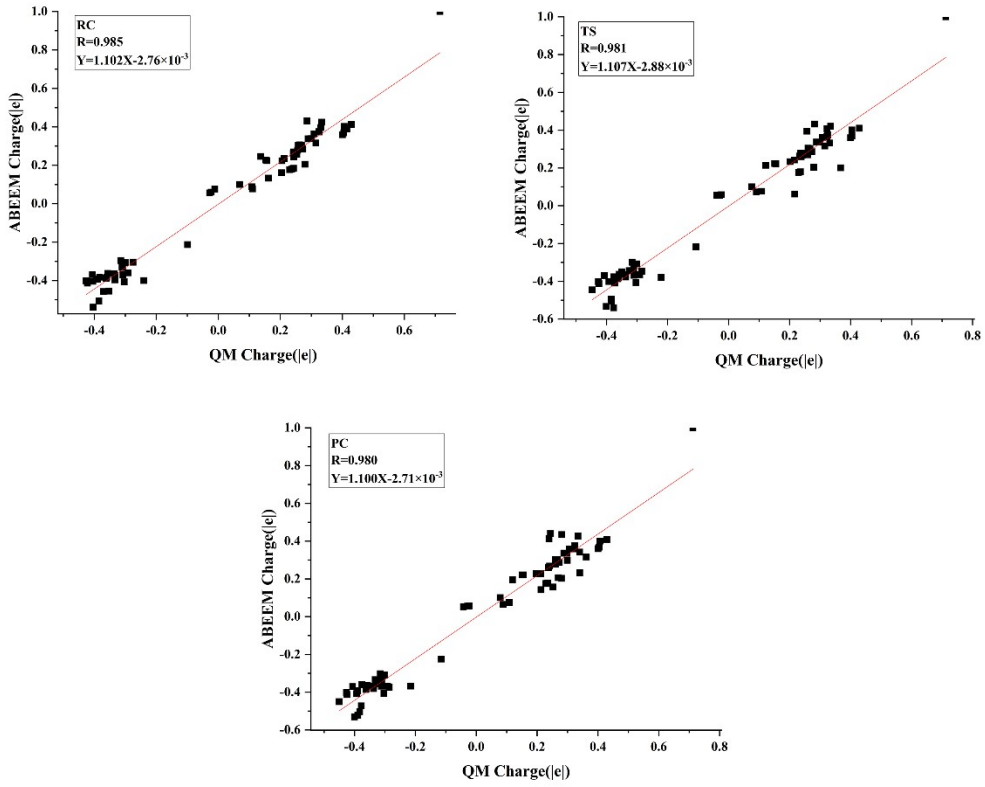

Fig. S4 The linear correlations of charge distributions of RC, TS and PC during deprotonation of X• in GGX(8-oxo-G) tetrad obtained by QM/MM(ABEEM) and QM methods.

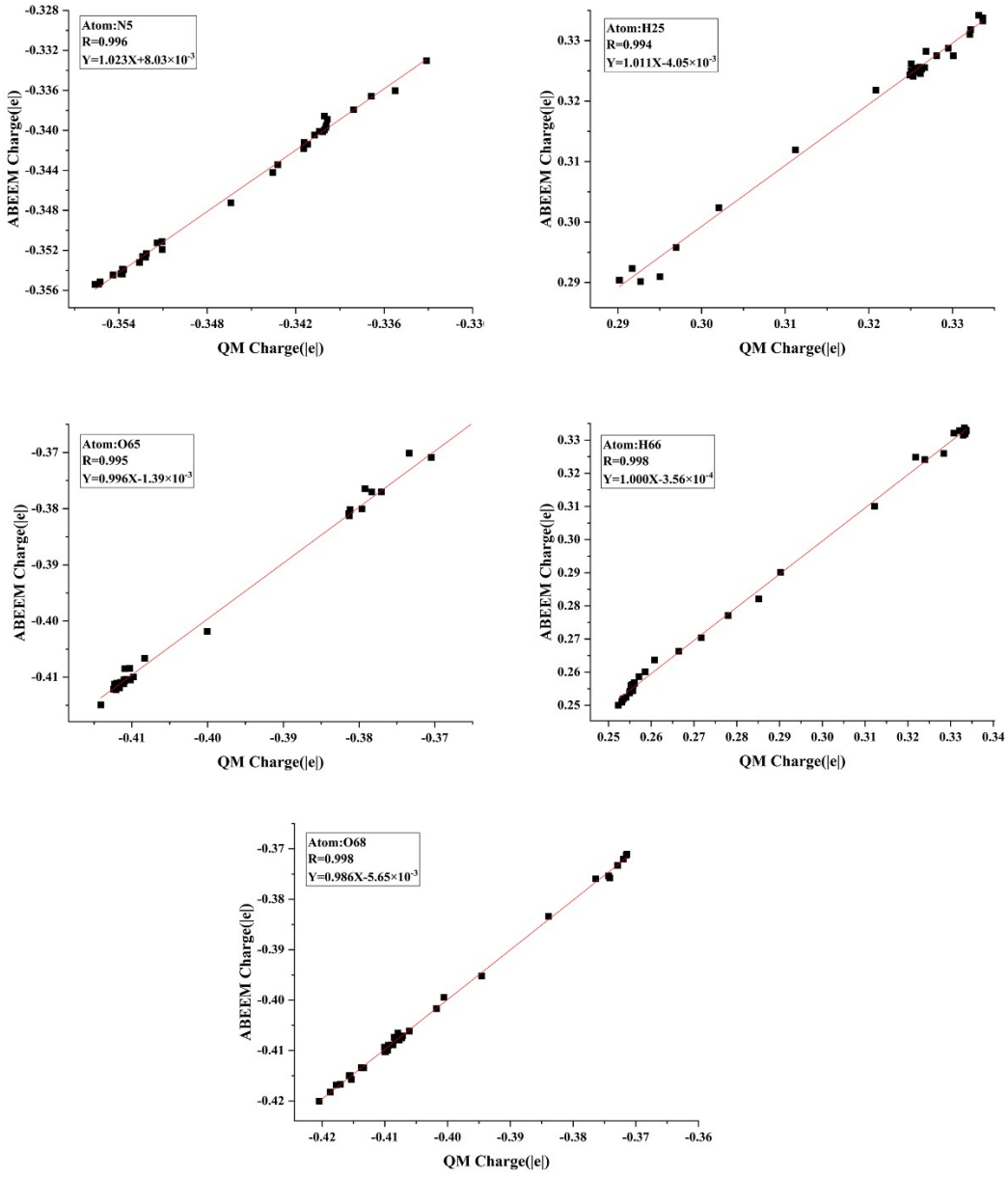

Fig. S5 The linear correlations of the atoms involved in bond-forming and bond-breaking calculated by QM/MM(ABEEM) and QM methods in the deprotonation process of $G^{\bullet+}$ in G-tetrad.

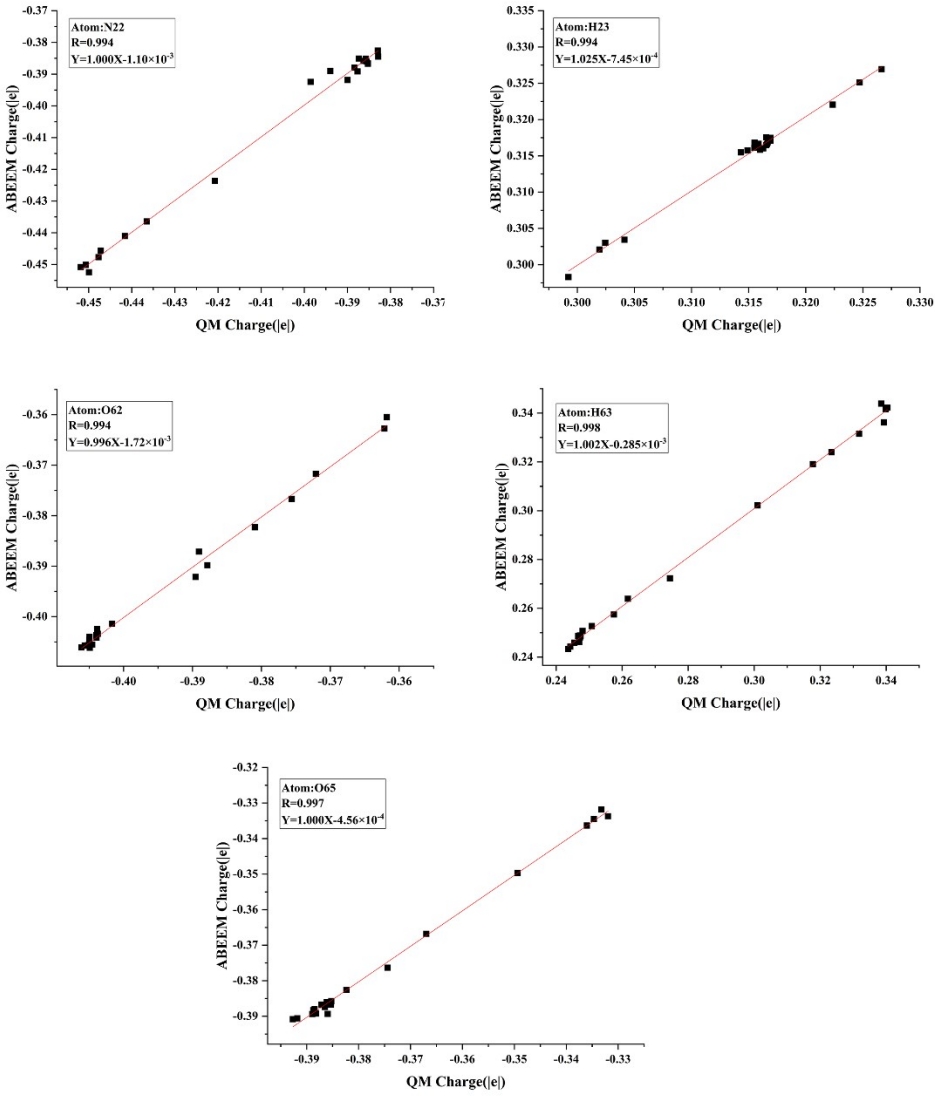

Fig. S6 The linear correlations of the atoms involved in bond-forming and bond-breaking obtained by QM/MM(ABEEM) and QM methods in the deprotonation process of X• in GGX(8-oxo-G) tetrad.

2 Position of proton in the optimized structures and variations of each site in the QM/MM(ABEEM) method

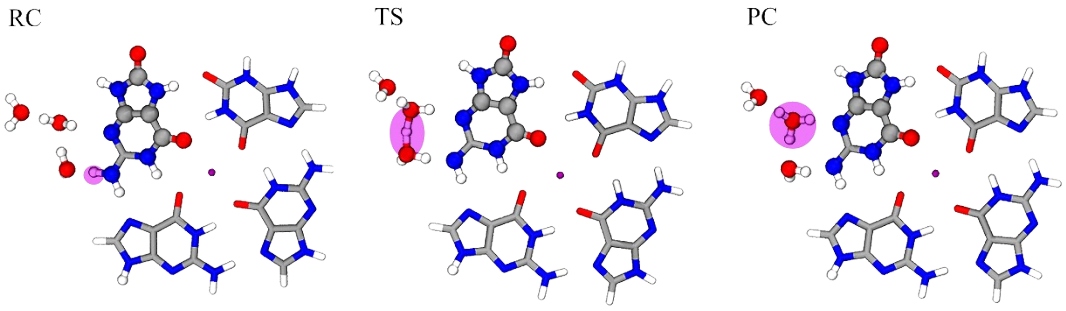

Fig. S7 The position of proton in the optimized structures of RC, TS, and PC in the deprotonation of 8-oxo-G$^{\bullet+}$ in GGX(8-oxo-G) tetrad. Sodium ion (purple sphere), nitrogen atom (blue sphere), oxygen atom (red sphere), carbon atom (grey sphere) and hydrogen atom (white sphere).

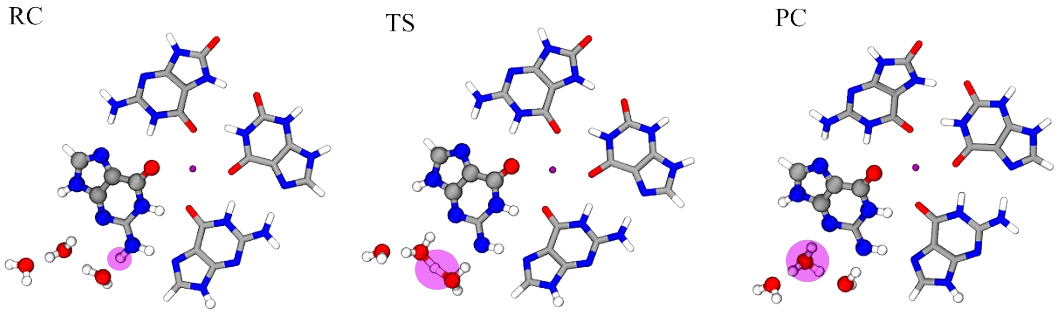

Fig. S8 The position of proton in the optimized structures of RC, TS, and PC in the deprotonation of G1$^{\bullet+}$ in GGX(8-oxo-G) tetrad. Sodium ion (purple sphere), nitrogen atom (blue sphere), oxygen atom (red sphere), carbon atom (grey sphere) and hydrogen atom (white sphere).

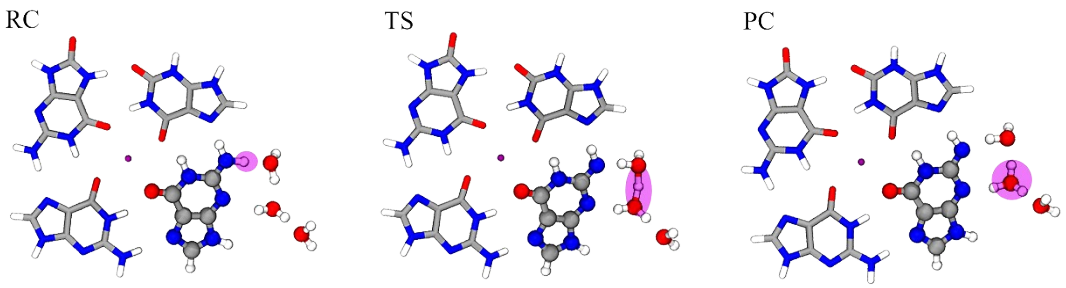

Fig. S9 The position of proton in optimized structures of RC, TS, and PC in the deprotonation of G2• in GGX(8-oxo-G) tetrad. Sodium ion (purple sphere), nitrogen atom (blue sphere), oxygen atom (red sphere), carbon atom (grey sphere) and hydrogen atom (white sphere).

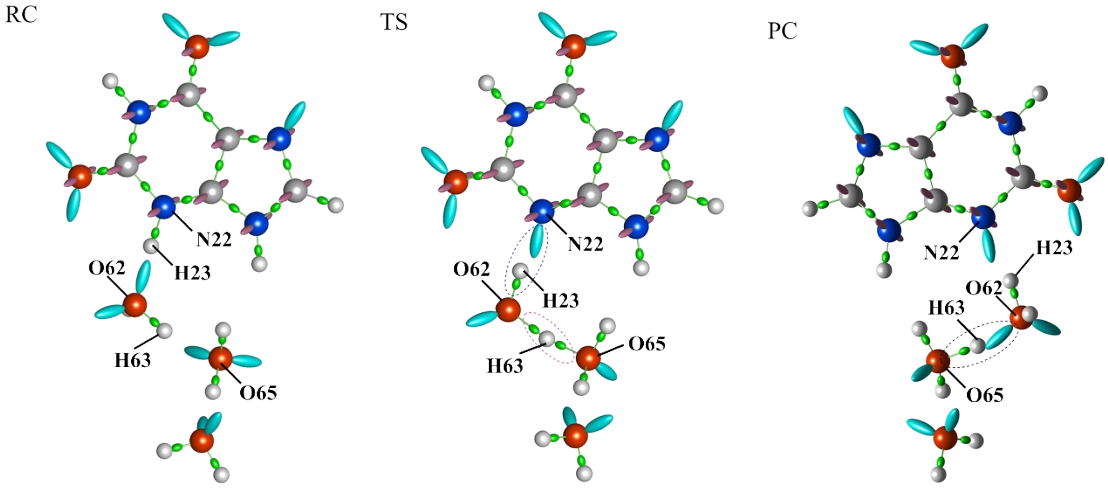

Fig. S10 Variations of each ABEEM site of RC, TS, and PC in the deprotonation of X• in GGX(8-oxo-G) tetrad.

3 The valence-state electronegativity piecewise function $\chi^*(r)$, charge distributions of 8-oxo-$G^{\bullet+}$, $G1^{\bullet+}$, and $G2^{\bullet}$ in GGX(8-oxo-G) tetrad, linear correlations at key stationary point calculated by QM/MM(ABEEM) and QM methods

Table S1 The $\chi^*(r)$ of N5 in the deprotonation of $G^{\bullet+}$ in G-tetrad (r represents the distance between N5 and H25)

Distances(Å)	Functions	Distances(Å)	Functions
$1.67 < r \leqslant 1.72$	$3.525-\frac{0.901}{1.0+\exp\frac{r-1.687}{0.069}}$	$1.59 < r \leqslant 1.67$	$3.674-\frac{0.036}{1.0+\exp\frac{r-1.112}{0.2}}$
$1.15 < r \leqslant 1.59$	$4.032-\frac{0.344}{1.0+\exp\frac{r-1.373}{0.117}}$	$1.09 < r \leqslant 1.15$	$4.898r+5.468$
$1.06 < r \leqslant 09$	$3.546-\frac{0.251}{1.0+\exp\frac{r-1.11}{0.01}}$		

Table S2 The $\chi^*(r)$ of H25 in the deprotonation of $G^{\bullet+}$ in G-tetrad (r represents the distance between H25 and O65)

Distances(Å)	Functions	Distances(Å)	Functions
$1.0 < r \leqslant 1.02$	$3.126-\frac{0.731}{1.0+\exp\frac{r-1.014}{0.012}}$	$1.02 < r \leqslant 1.05$	$7.273r+5.358$
$1.05 < r \leqslant 1.37$	$21.523r^2-57.144r+39.25$	$1.37 < r \leqslant 1.54$	$1.755-\frac{1.501}{1.0+\exp\frac{r-1.490}{0.301}}$
$1.54 < r \leqslant 1.60$	$2.44-\frac{0.79}{1.0+\exp\frac{r-1.58}{0.301}}$		

Table S3 The $\chi^*(r)$ of O65 in the deprotonation of $G^{\bullet+}$ in G-tetrad (r represents the distance between O65 and H25)

Distances(Å)	Functions	Distances(Å)	Functions
$1.0 < r \leqslant 1.02$	$4.2-\frac{2.001}{1.0+\exp\frac{r-1.005}{0.008}}$	$1.02 < r \leqslant 1.05$	$2.545r+5.917$
$1.05 < r \leqslant 1.37$	$9.178r^2-16.45r+39.25$	$1.37 < r \leqslant 1.54$	$4.620-\frac{2.711}{1.0+\exp\frac{r-1.5}{0.355}}$
$1.54 < r \leqslant 1.60$	$3.58-\frac{0.401}{1.0+\exp\frac{r-1.58}{0.075}}$		

Table S4 The $\chi^*(r)$ of H66 in the deprotonation of $G^{\bullet+}$ in G-tetrad (r represents the distance between H66 and O68)

Distances(Å)	Functions	Distances(Å)	Functions
$1.11 < r \leqslant 1.14$	$2.09-\frac{0.001}{1.0+\exp\frac{r-1.59}{0.118}}$	$1.14 < r \leqslant 1.20$	$0.406r+1.981$
$1.20 < r \leqslant 1.49$	$3.098-\frac{0.820}{1.0+\exp\frac{r-1.455}{0.022}}$	$1.49 < r \leqslant 1.54$	$2.425-\frac{0.455}{1.0+\exp\frac{r-1.59}{0.118}}$

Table S5 The $\chi^*(r)$ of O68 in the deprotonation of $G^{\bullet+}$ in G-tetrad (r represents the distance between O68 and H66)

Distances(Å)	Functions	Distances(Å)	Functions
$1.11 < r \leqslant 1.14$	$2.09-\frac{0.001}{1.0+\exp\frac{r-1.59}{0.118}}$	$1.14 < r \leqslant 1.20$	$1.375r+1.416$
$1.20 < r \leqslant 1.49$	$-0.707r^2+3.512r-0.051$	$1.49 < r \leqslant 1.63$	$4.268-\frac{1.5}{1.0+\exp\frac{r-1.55}{0.9}}$
$1.63 < r \leqslant 1.7$	$3.2-\frac{0.19}{1.0+\exp\frac{r-1.667}{1.105}}$		

Table S6 The $\chi^*(r)$ of N22 in the deprotonation of X• in GGX(8-oxo-G) tetrad (r represents the distance between N22 and H23)

Distances(Å)	Functions	Distances(Å)	Functions
1.06<r≤1.0725	$3.193-\frac{0.081}{1.0+\exp\frac{r-1.070}{0.002}}$	1.484<r≤1.60	2.654
1.0725<r≤1.08	$3.740+\frac{0.289}{1.0+\exp\frac{r-1.075}{0.080}}$	1.60<r≤1.72	$3.480-\frac{1.591}{1.0+\exp\frac{r-1.656}{0.005}}$
1.08<r≤1.484	$-1.232r^2+4.369r+0.628$		

Table S7 The $\chi^*(r)$ of O65 in the deprotonation of X• in GGX(8-oxo-G) tetrad (r represents the distance between H63 and O65)

Distances(Å)	Functions	Distances(Å)	Functions
1.58<r≤1.71	$3.207+\frac{0.095}{1.0+\exp\frac{r-1.560}{1.100}}$	1.12<r≤1.15	$-0.764r+3.378$
1.51<r≤1.58	$0.352r+2.983$	1.11<r≤1.12	$9.062r-7.552$
1.15<r≤1.51	$3.570-\frac{3.889}{1.0+\exp\frac{r-1.012}{0.127}}$		

Table S8 The $\chi^*(r)$ of H23 in the deprotonation of X• in GGX(8-oxo-G) tetrad (r represents the distance between H23 and O62)

Distances(Å)	Functions	Distances(Å)	Functions
1.57<r≤1.60	$2.312+\frac{0.790}{1.0+\exp\frac{r-1.573}{0.200}}$	1.02<r≤1.11	$-9.536r+12.697$
1.36<r≤157	$2.432+\frac{0.012}{1.0+\exp\frac{r-1.560}{0.226}}$	1.009<r≤1.02	$3.730r-1.216$
1.45<r≤1.56	$10.020r^2-31.025r+26.368$	1.00<r≤1.009	$23.121r-20.758$
1.11<r≤1.45	$19.472r^2-50.990r+35.470$		

Table S9 The $\chi^*(r)$ of H63 in the deprotonation of X• in GGX(8-oxo-G) tetrad (r represents the distance between H63 and O65)

Distances(Å)	Functions	Distances(Å)	Functions
1.52<r≤1.72	$2.400+\frac{0.415}{1.0+\exp\frac{r-1.590}{0.118}}$	1.3<r≤1.35	$20.269r^2-51.565r+35.030$
1.35<r≤1.49	$2.970r-1.734$	1.11<r≤1.30	$0.647r+1.937$

Table S10 The $\chi^*(r)$ of O62 in the deprotonation of X• in GGX(8-oxo-G) tetrad (r represents the distance between H23 and O62)

Distances(Å)	Functions	Distances(Å)	Functions
1.55<r≤1.60	$3.525-\frac{0.251}{1.0+\exp\frac{r-1.580}{0.075}}$	1.015<r≤1.11	$3.181+\frac{1.105}{1.0+\exp\frac{r-1.032}{0.005}}$
1.37<r≤155	$4.400-\frac{2.211}{1.0+\exp\frac{r-1.500}{0.355}}$	1.0<r≤1.015	$3.840+\frac{0.276}{1.0+\exp\frac{r-1.025}{0.300}}$
1.11 <r≤1.37	$5.949r-3.199$		

Table S11 Charge (|e|) distributions of 8-oxo-G$^{\bullet+}$ in GGX(8-oxo-G) tetrad

Structure	RC	TS	PC
G1	0.14	0.10	0.09
G2	0.11	0.11	0.11
X	0.13	0.13	0.13
8-oxo-G$^{\cdot+}$	0.80	---	---
8-oxo-G (-H)$^{\cdot}$	---	0.14	0.12
W1	0.04	---	0.15
W1···H···W2	---	0.73	---
W2	0.01	---	---
W2···H	---	---	0.59
W3	0.05	0.09	0.10
Na^+	0.71	0.71	0.71

Table S12 Charge (|e|) distributions of G1$^{\bullet+}$ in GGX(8-oxo-G) tetrad

Structure	RC	TS	PC
8-oxo-G	0.06	0.05	0.05
G2	0.16	0.10	0.10
X	0.16	0.15	0.15
G1$^{\cdot+}$	0.63	---	---
G1(-H)$^{\cdot}$	---	0.16	0.14
W1	0.05	---	0.16
W1···H···W2	---	0.74	---
W2	0.01	---	---
W2···H	---	---	0.59
W3	0.05	0.09	0.10
Na^+	0.71	0.71	0.71

Table S13 Charge (|e|) distributions of G2• in GGX(8-oxo-G) tetrad

Structure	RC	TS	PC
G1	0.10	0.11	0.11
8-oxo-G	0.99	0.04	0.04
X	0.19	0.15	0.15
$G2^{\cdot}$	-0.09	---	---
$G2(-H)^{\cdot}$	---	0.16	0.14
W1	0.03	---	0.16
W1···H···W2	---	0.74	---
W2	0.01	---	---
W2···H	---	---	0.59
W3	0.04	0.09	0.10
Na^{+}	0.72	0.71	0.71

Table S14 The linear correlations at each stationary point calculated by QM/MM(ABEEM) and QM methods in the deprotonation of $G^{\bullet+}$ in G-tetrad

Local conservation condition 1		Local conservation condition 2		Local conservation condition 3	
Reaction path	R	Reaction path	R	Reaction path	R
1	0.98	46	0.97	53	0.97
4	0.98	50	0.97	57	0.97
7	0.98	-	-	59	0.97
10	0.98	-	-	63	0.97
13	0.98	-	-	-	-
16	0.98	-	-	-	-
19	0.98	-	-	-	-
22	0.98	-	-	-	-
25	0.98	-	-	-	-
28	0.98	-	-	-	-
31	0.98	-	-	-	-
37	0.98	-	-	-	-
40	0.98	-	-	-	-
43	0.98	-	-	-	-

Table S15 The linear correlations of at each stationary point calculated by QM/MM(ABEEM) and QM methods in the deprotonation of X• in GGX(8-oxo-G) tetrad

Local conservation condition 1		Local conservation condition 2		Local conservation condition 3	
Reaction path	R	Reaction path	R	Reaction path	R
1	0.98	46	0.97	53	0.98
4	0.98	50	0.97	57	0.98
7	0.98	-	-	59	0.98
10	0.98	-	-	63	0.98
13	0.98	-	-		
16	0.98	-	-		
19	0.98	-	-	-	-
22	0.98	-	-	-	-
25	0.98	-	-	-	-
28	0.98	-	-	-	-
31	0.98	-	-	-	-
37	0.98	-	-	-	-
40	0.98	-	-	-	-
43	0.98	-	-	-	-